

Ångström-Precision Optical Traps and Applications*

Thomas T. Perkins^{1,2}

¹JILA, National Institute of Standards and Technology and University of Colorado, Boulder, Colorado 80309; email: tperkins@jila.colorado.edu

²Department of Molecular, Cellular, and Developmental Biology, University of Colorado, Boulder, Colorado 80309

Annu. Rev. Biophys. 2014. 43:279–302

First published online as a Review in Advance on April 24, 2014

The *Annual Review of Biophysics* is online at biophys.annualreviews.org

This article's doi: 10.1146/annurev-biophys-042910-155223

*This is a work of the US Government and is not subject to copyright protection in the United States.

Keywords

optical tweezers, single-molecule force spectroscopy, DNA, molecular motor, RNA polymerase

Abstract

Single-molecule optical-trapping experiments are now resolving the smallest units of motion in biology, including 1-base-pair steps along DNA. This review initially concentrates on the experimental problems with achieving 1-Å instrumental stability and the technical advances necessary to overcome these issues. Instrumental advances are complemented by insights in optical-trapping geometry and single-molecule motility assay development to accommodate the elasticity of biological molecules. I then discuss general issues in applying this measurement capability in the context of precision measurements along DNA. Such enhanced optical-trapping assays are revealing the fundamental step sizes of increasingly complex enzymes, as well as informative pauses in enzymatic motion. This information in turn is providing mechanistic insight into kinetic pathways that are difficult to probe by traditional assays. I conclude with a brief discussion of emerging techniques and future directions.

Contents

INTRODUCTION	280
EXPERIMENTAL TECHNIQUES AND ADVANCES	282
Mechanically Measuring the Length of a Single Molecule	283
Brownian Motion Limits Spatiotemporal Resolution	283
Eliminating Mechanical Drift Using an Optically Based Reference Frame	286
Compliance Correction and Its Elimination	286
Different Biological Assays Yield Different Size Signals	288
Quantifying Steps	290
Detection and Stabilization to One Ångström in Three Dimensions	291
APPLICATIONS TO SELECT MOLECULAR MOTORS	293
Pauses in Motion Are as Informative as Steps	293
Mechanistic Insight from Improved Spatiotemporal Resolution	294
EMERGING TECHNICAL ADVANCES AND NEXT STEPS	296
SUMMARY	297

INTRODUCTION

One of the hallmarks of life is motion. At the smallest level, this motion is performed by molecular motors. Kinesin walks along microtubules for vesicular transport, and myosin pushes on actin filaments for muscle contraction. A less obvious, but still critical, molecular motor is RNA polymerase (RNAP), which moves along DNA as it makes RNA. Indeed, many of the enzymes involved in the central dogma of molecular biology are molecular motors (e.g., helicases, polymerases, the ribosome). Such directed motion necessarily consumes energy. In general, these molecular motors utilize the energy stored in nucleotide triphosphates (NTPs) to move along their underlying template (**Figure 1a**). Traditional biochemical and biophysical studies have taught us numerous critical facts about each of these systems, including their kinetic rates and critical residues necessary for catalysis (5).

To fully understand how these motors work, we need to answer additional questions, such as the following: What is a motor's step size? How much force does it generate? To answer these and other important questions, scientists have spent the past two decades increasing the precision of a variety of physical techniques to probe single molecules (32, 60, 71), including single-molecule fluorescence, single-molecule fluorescence resonance energy transfer (FRET), magnetic tweezers, atomic force microscopy (AFM), and optical traps. Although each of these techniques has its own strengths and limitations, optical traps have proven particularly well suited to studies of molecular motors.

Two early triumphs in the field were resolving the individual steps of the canonical motor proteins, kinesin and myosin. The measured step size of kinesin was 8 nm, corresponding to the fundamental repeating unit of the microtubule (82). The initial step size of myosin was ~10 nm (27), but it was quickly revised to ~5 nm using improved analysis (55).

Early trapping work also focused on DNA. Researchers investigated questions in polymer physics by manipulating and visualizing individual DNA molecules (20, 65–67, 77). Single-molecule studies of DNA-based molecular motors were also developed. Initial investigations focused on RNAP (91, 96), DNA polymerase (DNAP) (94), and RecBCD, a DNA helicase (6).

RNAP: RNA polymerase

AFM: atomic force microscope

DNAP: DNA polymerase

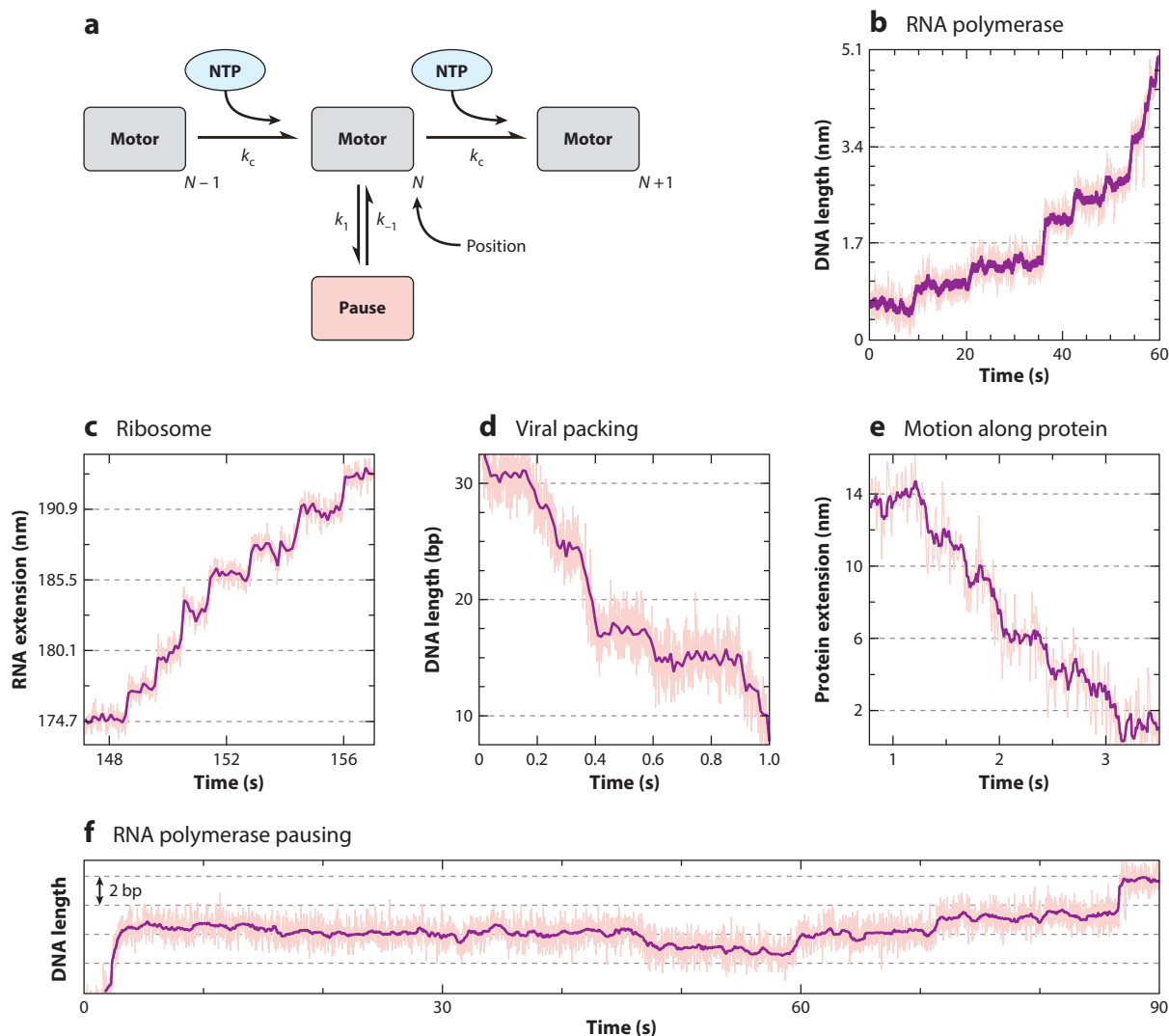


Figure 1

Measuring the motion of individual molecular motors. (a) A simplified kinetic diagram of a molecular motor showing an off-pathway pause. (b) Record of RNA polymerase (RNAP) motion along DNA showing 1-bp (0.34-nm) steps. Panel adapted with permission from Reference 1. (c) Record of ribosomal motion along RNA showing 1-codon steps (3 nucleotides), which in this assay are amplified to 2.7-nm steps (see **Figure 6b**). Panel adapted with permission from Reference 93. (d) Record of the DNA packaging motor from bacteriophage $\phi 29$ pulling in the DNA in 2.5-bp steps. Panel adapted with permission from Reference 52. (e) Record of ClpX, an adenosine triphosphate (ATP)-powered protease, moving along a protein substrate in discrete translocations of four to eight amino acids per step. Panel adapted with permission from Reference 3. (f) Record of RNAP motion along DNA showing forward steps interspersed with a long pause associated with 1 bp of backwards motion. Adapted from Reference 1. High-bandwidth data (pink) are smoothed to generate traces with improved spatial precision (dark purple) at the loss of temporal resolution. Abbreviations: N , position index of the molecular motor along its polymeric substrate; k_c , catalytic rate for forwards translocation; k_1 and k_{-1} , kinetic rates into and out of a paused state, respectively NTP, nucleotide triphosphate.

bp: base pair

Resolution:

a localization precision often used in the context of “resolving” steps of molecular motors, distinctly different than diffraction-limited resolution

An immediate question arose: Could one resolve the stepping of an individual enzyme moving along DNA? The fundamental building block of double-stranded (ds) DNA is the base pair (bp), which is 3.4 Å in length along DNA’s helical backbone and much smaller than the Brownian motion and the drift in these early instruments. To confidently measure a step this small, an optical trap with ~ 1 -Å precision and stability was needed. However, achieving such spatially precise measurements in liquid at room temperature posed a significant instrumental challenge. After a decade of insight and instrumental advancement, Abbondanzieri et al. (1) successfully measured the stepping of individual RNAP (**Figure 1b**). The techniques developed in this pioneering work are being extended and improved upon (17, 53) to observe individual steps of an increasingly wide range of molecular motors, including ribosomal motion along RNA (93) (**Figure 1c**), DNA packaging into bacteriophage capsids (**Figure 1d**) (52), and force-induced protein unfolding by proteases moving along proteins (**Figure 1e**) (3, 49). Extended pauses in molecular motion are also detected with 1-bp spatial precision (**Figure 1f**) (1).

This review focuses on several developments needed to make Ångström-scale measurements with optical traps and on general issues that arise in applying this measurement capability. There are numerous methods to build and calibrate traps, which have already been well reviewed (45, 54, 59, 62, 80, 86). Additionally, there are excellent reviews on biological insight derived using high-resolution optical traps on diverse single-molecule systems (4, 14, 15, 35, 37, 85, 97, 100). For specificity, I focus on nucleic acid-based molecular motors.

EXPERIMENTAL TECHNIQUES AND ADVANCES

In the following sections, I briefly review the basic components of a modern high-performance optical trap, how to measure the length of biopolymers using optical traps, and how Brownian motion affects their spatiotemporal resolution. Finally, I discuss the challenges and technical advances in achieving Ångström-scale precision and stability in optical traps.

Optical traps typically consist of a high-numerical aperture (NA) microscope objective, a condenser lens, an electronically controllable piezoelectric (PZT) translation stage, and a laser (Figure 2a). The high-NA objective tightly focuses the laser beam to a diffraction-limited spot. The condenser collects the forward-scattered light and projects it onto a position-sensitive

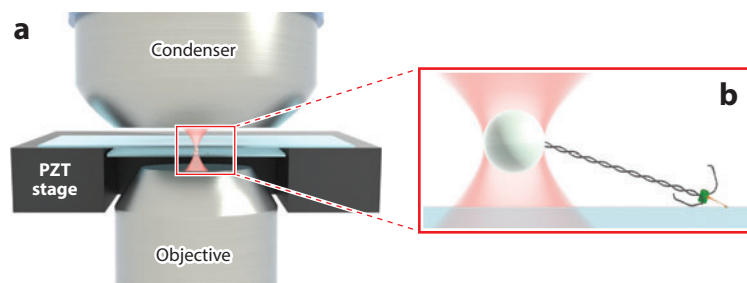


Figure 2

(a) Schematic of an optical trap showing the laser beam being focused by a high-numerical aperture objective and a condenser lens collecting the transmitted (forward-scattered) light. A three-axis nanopositioning piezoelectric (PZT) translation stage facilitates high-precision positioning of the sample relative to the trap. (b) Enlarged inset showing the optical trap measuring the motion of a surface-bound enzyme along DNA. Both the trap and the surface can undergo unwanted motion, degrading high-precision measurements of enzymatic motion.

detector, often a quadrant photodiode (QPD). The PZT stage provides for precise control of the sample relative to the trap in three dimensions (3D), typically with subnanometer precision.

Although most high-resolution optical-trapping studies are now decoupled from the surface (1, 16, 52, 78, 98), the original assays for studying myosin, kinesin, RNAP, and DNAP were coupled to the surface, either through a cover slip (27, 82, 96) or a bead held in a micropipette (94). For specificity, I focus on the tethered-bead assay developed for studying DNA-based molecular motors, such as RNAP (95). As shown in **Figure 2b**, mechanical studies of motor proteins are a molecular tug of war. One of the major milestones in the application of optical traps to biology was determining the force–velocity (F – v) relationship for RNAP (91), kinesin (81, 89), and DNAP (94).

Mechanically Measuring the Length of a Single Molecule

To be broadly useful, the motions of enzymes along various kinds of substrates need to be characterized in their natural units. For velocities along DNA, RNA, and protein, these would be base pairs (bp), nucleotides (nt), and amino acids (aa) per second, respectively. However, the raw measurement is a voltage (V_x) determined by the light landing on a QPD (**Figure 3**). A series of steps are needed to convert V_x to the number of monomers in the chain. One first converts V_x to bead position (x_{bd}) and then converts x_{bd} into a polymer extension (x_{DNA}). A sensitivity calibration maps V_x into x_{bd} . This conversion is simplified when the calibration curve is insensitive to small displacements of the trapping beam, a benefit of back-focal-plane (BFP) detection (88); BFP detection measures x_{bd} relative to the laser focus, not an external reference frame. Electronic normalization of V_x by the total light falling on the QPD further improves the measurement precision by suppressing the effects of intensity fluctuations.

The geometry of the assay is critical to converting x_{bd} into the extension of the DNA (x_{DNA}) (**Figure 3**). Extension is force dependent, so geometric considerations are particularly important when computing x_{DNA} and F along the stretching axis of a surface-coupled assay (92). Biopolymers are nonlinear springs with a force–extension curve well described by the worm-like chain (WLC) model (8, 50, 92) (**Figure 3**). This nonlinearity leads to most high-resolution measurements being done at higher forces ($F > 6$ pN) for a more precise determination of the force-independent length of a polymer, called its contour length (L). A pair of experimental measurements (F , x_{DNA}) leads to a unique value of L via the WLC model and the DNA's persistence length, its bending stiffness. The persistence length of dsDNA is ~ 50 nm (33) at physiological salt concentrations, but this length can appear smaller when analyzing shorter DNA molecules with the traditional WLC model (74). Finally, the contour length is converted into the number of monomers in the chain based upon the rise per monomer (0.34 nm bp^{-1}) for dsDNA (**Figure 3**).

Brownian Motion Limits Spatiotemporal Resolution

What prevented early studies from measuring the step size of RNAP? The key issue was not the sensitivity of laser-based detection of bead motion; Denk et al. (25) demonstrated a spatial sensitivity to bead motion of $0.01 \text{ \AA Hz}^{-0.5}$ in 1990. Rather, the limit was developing Ångström-scale stability over sufficiently long times to average the large Brownian motion of an optically trapped bead (**Figure 4a**). The lack of long-time scale stability was a well-documented problem. Indeed, the sensitive instrument developed by Denk et al. (25) was limited by drift that was three orders of magnitude larger at 1 Hz than the reported spatial sensitivity at higher frequencies.

Brownian motion has a zero mean, so the key tradeoff in all high-resolution optical-trapping measurements is to compromise temporal resolution for improved spatial precision by averaging (**Figure 4b**). For simplicity, I discuss measuring an isolated trapped bead before discussing coupled systems incorporating biological molecules. The standard deviation (σ_x) in x_{bd} is set by k_{trap} via the

QPD: quadrant photodiode

nt: nucleotide

aa: amino acid

Extension: the end-to-end distance of a stretched polymer; extension is a force-dependent property for which higher forces lead to higher extensions

Worm-like chain (WLC) model: A polymer physics model that describes the elasticity of biopolymers and is used to deduce L from F and x_{DNA}

Contour length (L): the force-independent distance along a polymer's backbone that is proportional to the number of monomers in the polymer

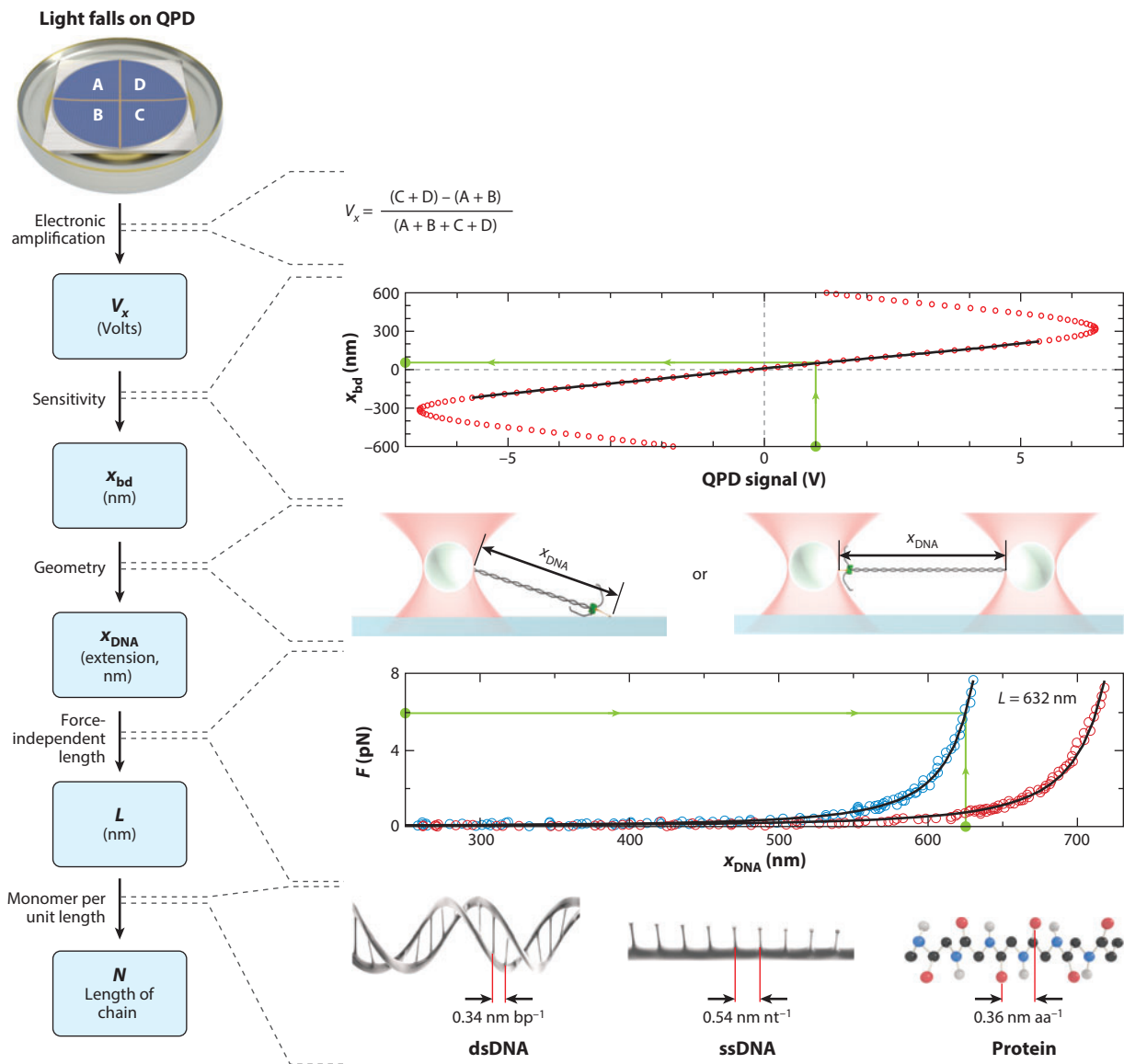


Figure 3

An overview showing how optical traps are used to determine the mechanical length of a DNA molecule, in particular, and a biopolymer, in general. The laser light is detected by a quadrant photodiode (QPD). This light is converted into a voltage (V_x). Prior calibration of the QPD to bead displacement (x_{bd}) enables conversion of V_x to x_{bd} via a calibration curve (*line*). The geometry of the assay—shown here as either a surface-coupled assay or a dual-trap assay—is necessary to determine the extension of the DNA (x_{DNA}). A quantitative description of the elasticity of the DNA by the worm-like chain model (*line*) enables the conversion of x_{bd} and the applied F to a force-independent length, called the contour length (L). Finally, this contour length, measured in nm, is converted into biologically relevant units: base pairs (bp), nucleotides (nt), or amino acids (aa), depending on the individual assay. Abbreviations: dsDNA, double-stranded DNA; ssDNA, single-stranded DNA.

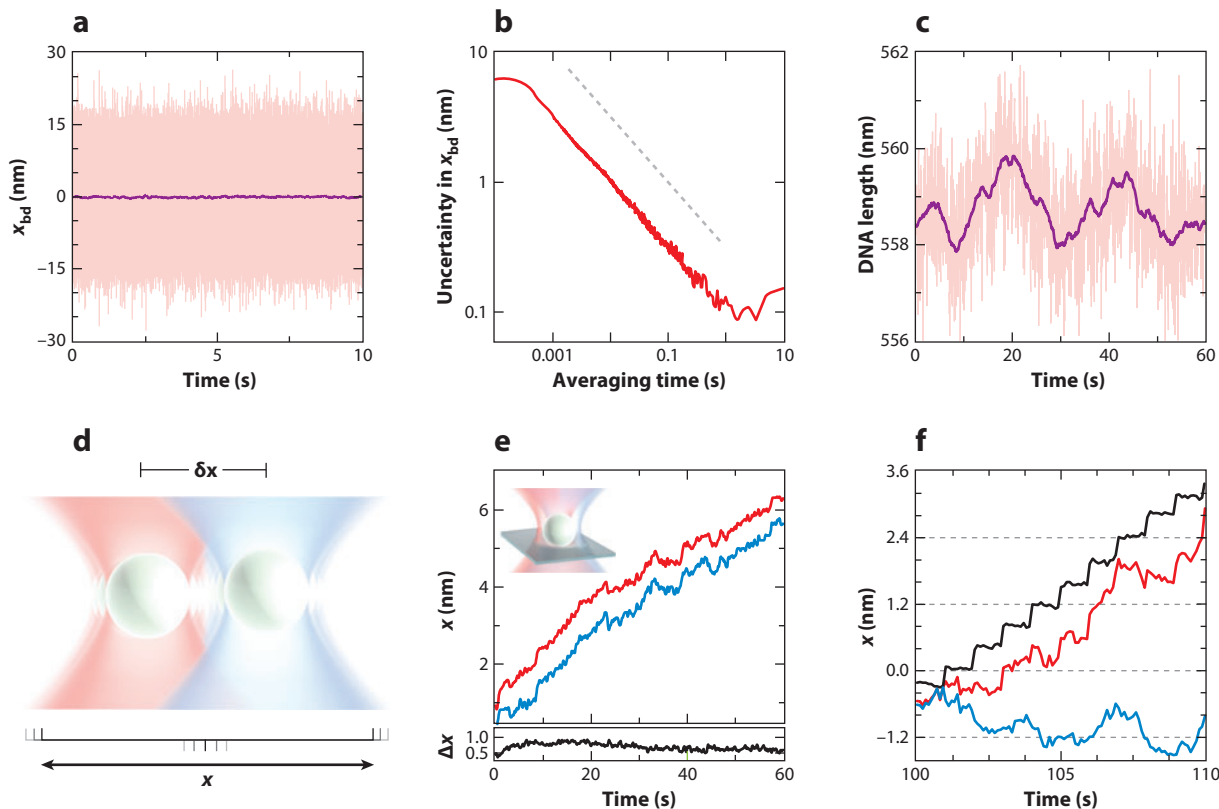


Figure 4

(a) Trace showing the significant Brownian motion on an isolated optically trapped bead ($k_{\text{trap}} = 0.11 \text{ pN nm}^{-1}$). The high-bandwidth data (pink, 15 kHz) were smoothed to 10 Hz [purple, 20 data points s^{-1} (based on the Nyquist frequency)]. The high-bandwidth data have a standard deviation of 5.9 nm. (b) Positional precision increases by averaging over longer periods. Technically, this panel plots the Allan variance (79). The gray dashed line has a slope consistent with averaging Brownian motion. Deviations away from this slope at longer averaging times shows instrumental noise limiting the ability to improve spatial precision at the cost of temporal resolution (23). (c) Record of DNA length in a surface-coupled optical-trapping assay showing the problem of resolving 1-bp motions, even in an environmentally regulated room, without additional steps (1, 12). Panel adapted with permission from Reference 12. (d) Two lasers form an optically based reference frame. The central idea is that common-mode motion is suppressed by making a differential measurement based upon the distance between the laser foci. (e) Record of two lasers (red and blue) measuring the same bead stuck to a cover slip. The difference between these two measurements (black) is stable to $\sim 0.5 \text{ nm}$ over 1 min and does not show the rapid transient motions seen in the individual position measurements. (f) Stage motion (blue) obscures detection of 4-Å steps of one laser (red). By computing the difference between the two (black), these 4-Å steps are clearly resolved. Traces displaced for clarity. Panel adapted with permission from Reference 61.

equipartition theorem: $\sigma_x^2 = k_B T / k_{\text{trap}}$. For a typical k_{trap} (0.11 pN nm^{-1}), σ_x is $\sim 6 \text{ nm}$, 60 times larger than the $1\text{-}\text{\AA}$ precision needed to resolve 1-bp steps. Averaging reduces Brownian motion, but the precision improves slowly, with the same scaling relation as the standard error in the mean has to the standard deviation $\sigma_x^{\text{SEM}} = \sigma_x / \sqrt{n}$, where n is the number of independent measurements. To be independent, such measurements must be separated by at least the correlation time of the bead motion. This time depends on k_{trap} and the bead radius; a typical time is $\sim 0.5 \text{ ms}$. Thus, it takes $\sim 2 \text{ s}$ to achieve a $1\text{-}\text{\AA}$ spatial precision, a time over which even modern highly stable optical-trapping instruments suffer from drift (Figure 4c) in the absence of additional drift-reduction techniques (1, 12). Instrumental drift is, therefore, a critical issue limiting the field.

Optically based reference frame:

a differential measurement scheme where the distance relative to two laser foci is measured rather than an absolute position

Instrumental drift is a general problem that can arise from a host of different causes, such as temperature fluctuations, electronic noise, and mechanical drift. At significant effort and cost, leading groups designed acoustically quiet, temperature-regulated rooms in the basements of buildings to address these issues. Moreover, they increased the stiffness and stability of the optical-trapping instruments themselves. Such next-generation surface-coupled optical traps in these specialized rooms showed subnanometer stability along DNA (58, 63), but they occasionally displayed spurious high-frequency motion with an estimated noise of 1.4 nm (4 bp) (64). The jump to measuring 1-bp motion along DNA awaited a set of additional insights.

Eliminating Mechanical Drift Using an Optically Based Reference Frame

The main limitation with surface-coupled assays is the stability of the surface. More generally, the surface and the optical trap can move relative to each other. Shaevitz et al. (75) solved this problem by decoupling the assay from the surface, similar to earlier work that visualized the polymer modes of taut DNA (67). In this dual-trap, or dumbbell, assay (**Figure 3**), two beads are trapped in two different traps; the RNAP is coupled to one bead, and the DNA is anchored to the other. As the RNAP moves along the DNA, the beads are pulled together. This assay led to enhanced long-term stability, achieving near base-pair resolution that led to insight into the pausing and backtracking of RNAP.

The central idea of the dual-trap assay is that the differential stability between two laser beams is significantly higher than the stability between one laser beam and a surface (**Figure 4d**). In this optically based reference frame, the motion of a common lens causes both beams to move an equal amount so that the distance between the trapped beads remains fixed and the perturbation is suppressed. This suppression is possible because, as discussed above, BFP detection measures the bead relative to the laser beam, not its absolute position in the microscope's field of view.

The stability of an optically based reference frame is probed by using two lasers to measure a common object (**Figure 4e**, inset). My lab demonstrated the use of a polystyrene bead melted to a cover slip as a fiducial mark to measure the motion of the surface. Both measurements showed the sample drifting at a rate of 0.1 nm s^{-1} , with occasional rapid jumps. This record is typical for a highly stable microscope in an acoustically quiet, temperature-regulated room (**Figure 4e**). The key result is that the difference between the two laser beams was stable to better than 0.5 nm over 60 s. More generally, this “two-beam, one-bead” assay is an excellent diagnostic tool for tracking down non-common-mode noise. Such non-common-mode noise is critical because it limits the stability of measurements relying upon an optically based reference frame.

Similarly, surface-based noise could be subtracted out in real time by making a differential measurement with a precision of 1 \AA in 1 ms (61). To simulate enzymatic steps along DNA, we moved one laser beam in a series of 4-\AA steps relative to the other. In the uncorrected record (**Figure 4f**), no steps were resolved. But, when the surface noise was subtracted, the resulting differential measurement showed well-resolved steps with a signal-to-noise ratio of 25 (**Figure 4f**). This work highlights the challenge of surface-based assays, as well as a path forward to achieving 1-bp resolution in such assays. More generally, it shows that Ångström-scale short-term precision can be complemented with excellent long-term stability.

Compliance Correction and Its Elimination

Interpreting high-resolution measurement of biological molecules requires understanding the effects of their elasticity upon mechanical measurements. Both the trap and the biomolecule act like springs. Moreover, their extensions are coupled during a measurement. When a DNA molecule

is stretched, the force increases, and both x_{DNA} and x_{bd} change (**Figure 5a**). This has important consequences. For instance, if k_{trap} is made very stiff to decrease Brownian motion, then most of the stretching occurs in the softer spring, the DNA. The net result is that Δx_{bd} , the actual observable, changes very little. Indeed, it is straightforward to show that increasing k_{trap} does not improve the ability to resolve steps along DNA, assuming a linear spring for the optical trap (12, 53).

This complication is called compliance. The original kinesin stepping paper incorporated a compliance correction of 19%, yielding a step size of 8.3 ± 0.2 nm, but this result required knowing the elasticity of kinesin (82). Visscher et al. (89) circumvented the compliance problem by moving the optical trap to maintain a constant x_{bd} using a fast feedback loop. This feedback maintained a constant force across the kinesin. As a result, kinesin's extension remained constant. In such a force clamp, the motion of the trap is then equal to the step size of the protein. This improved assay also yielded an 8-nm step size and facilitated F - v analysis by allowing long records at constant F (89). Force clamps are now widely used in high-resolution stepping assays.

Compliance is still an issue within the update cycle of a force-clamp feedback loop, and the reduction in Δx_{bd} remains. Moreover, because a micron-long DNA molecule is much more elastic than a single kinesin, the attenuation in Δx_{bd} is much larger for measuring RNAP motion along DNA. Quantitatively, this attenuation is given by $k_{\text{DNA}}/(k_{\text{DNA}} + k_{\text{trap}})$ where k_{DNA} is the effective stiffness determined by the slope of the force-extension curve at a given F .

Greenleaf et al. (31) developed a novel solution to this problem called a passive force clamp. They pulled a bead out to the maximum F exerted by the optical trap (**Figure 5b**). At this maximum, small variations in x_{bd} leave F unchanged. Hence, k_{trap} is equal to 0 even though a significant F is applied. This trapping geometry eliminates the compliance correction and leads to the largest Δx_{bd} per step—an important issue when trying to measure very small steps.

The final hurdle to measuring 1-bp steps of RNAP was further suppression of low-frequency (<0.3 Hz) noise. This suppression was achieved by replacing the air surrounding the optics with helium to minimize beam pointing fluctuations caused by air currents (1). The tenfold reduction in the difference between the index of refraction of the gas and that of a vacuum led to a more than tenfold reduction in the integrated positional noise at 0.1 Hz. With this improved performance, Abbondanzieri et al. (1) resolved 1-Å steps of a trapped bead that stayed in register over approximately eight steps (**Figure 5c**). They next showed their ability to resolve 1-bp steps when using a DNA stretched to a high force (27 pN) (**Figure 5d**). The strong trap was moved in a series of 3.4-Å steps while monitoring x_{bd} in the weak, constant-force trap. The signal-to-noise ratio for detecting these larger steps is nominally identical to that for detecting 1-Å steps of a trapped bead alone. In other words, steps in a biological assay were threefold harder to resolve than for a trapped bead. The additional elements, such as the DNA, protein linkages to the beads, and the other optical trap, add compliance and complexity. The important lesson is that showing that an isolated trapped bead can resolve 3.4-Å motion is necessary but not sufficient for resolving 1-bp steps in a biological assay.

There are an increasing number of instruments around the world that can measure at or near resolutions of 1 bp (12, 17, 22, 53, 76). These instruments do not use a helium buffer gas. To reduce low-frequency noise, they decrease the fraction of the beam path over which the lasers are not colinear. However, the long-term stability of the helium system is still unrivaled in a biological assay. Long pauses of RNAP can be stable to 1-bp over time periods as long as ~ 30 s (**Figure 1f**). Further advances in instrumentation are ongoing and include analyzing the differential motion between beads in the dual-trap assay for improved temporal resolution (53) and changing the trapping laser wavelength to decrease thermal heating and photo-induced damage (17). Ångström-scale noise at low frequencies (<0.3 Hz) still limits most instruments and remains challenging to eliminate.

Compliance correction:

a correction to the measured bead displacement to yield the actual biological motion, after compensating for the elasticity of the biomolecule and the optical trap

Force clamp:

a process by which the force applied across a biological molecule or assay is held constant, typically by active feedback

ssDNA:

single-stranded DNA

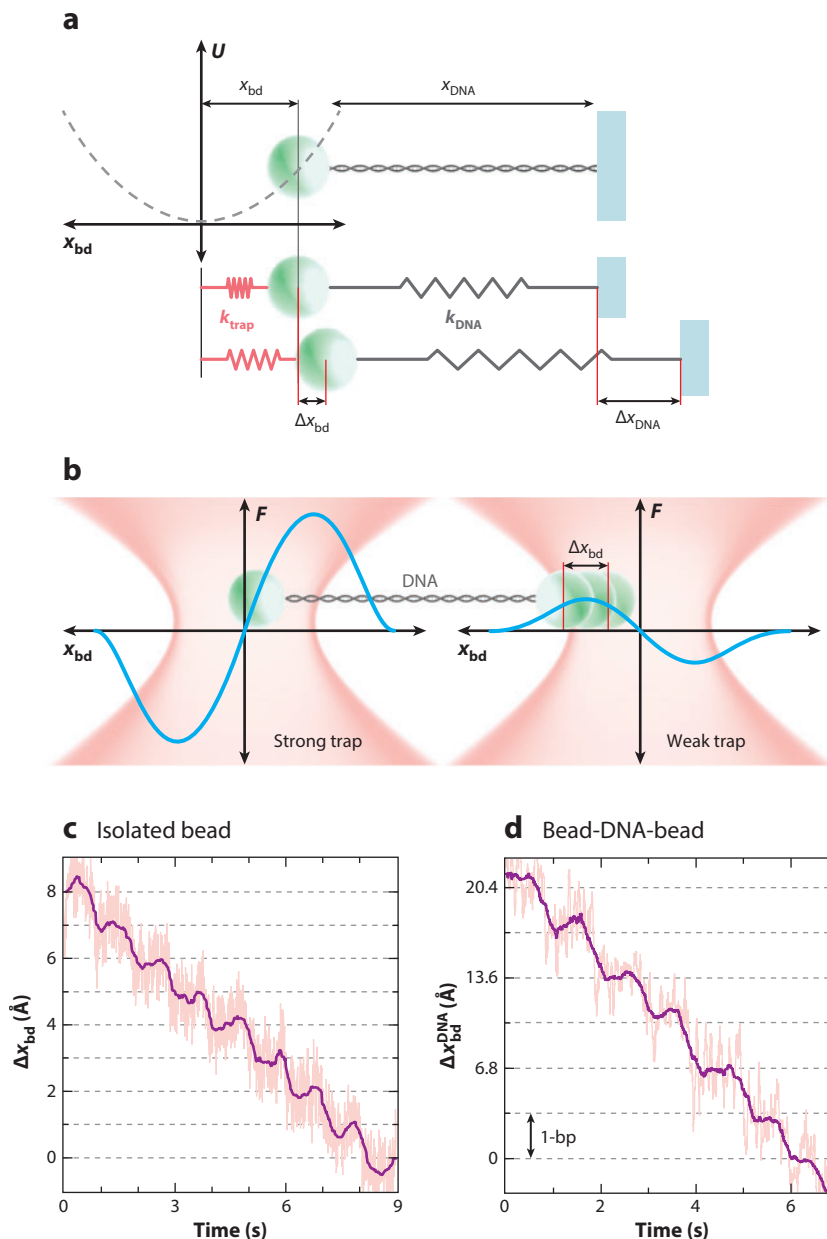
dsDNA:

double-stranded DNA

Different Biological Assays Yield Different Size Signals

Helicases unwind DNA and RNA. DNA polymerase converts single-stranded (ss) DNA to double-stranded (ds) DNA. Researchers are exploiting these different enzymatic functions to measure enzymatic motion using novel biological assays. The resulting measured step size is assay dependent.

The standard molecular motor assay is a tug-of-war assay in which the enzyme is anchored to one surface (bead or cover slip), and the distal end of the DNA is attached to a bead. In this assay,



a 1-bp motion along DNA leads to a ΔL of 3.4 Å (**Figure 6a**). Helicases can be studied using the same geometry (64). A larger signal can be achieved using a hairpin-unwinding assay because one base pair of enzymatic motion leads to two nucleotides being stretched (**Figure 6b**), similar to the assay for unfolding single RNA molecules (48). The total increase of L in this assay is 10.8 Å, more than threefold larger than the 3.4-Å increase in L in the tug-of-war assay. This amplification arises because two nucleotides are released, and the rise per nucleotide (5.4 Å) is larger than the rise per base pair (3.4 Å). Dumont et al. (26) implemented this geometry to study the RNA helicase NS3 and detected discrete steps in its motion. More generally, the unwinding assay is an excellent method to study helicases, some DNA polymerases (56), and even the ribosome (93), as long as the enzyme can initiate unwinding without access to a free end of the DNA or RNA.

Measurement of enzymatic motion can also be based on the difference between the elastic properties of ssDNA and dsDNA (**Figure 6c**). Wuite et al. (94) exploited this difference to measure the enzymatic activity of DNAP. In this assay, the formation of 1 bp from 1 nt leads to a ΔL of 2 Å. This assay enabled the measurement of the F - v relation of T7 DNAP, although it has yet to be used to resolve individual steps of DNAP. One limitation of this assay is its low sensitivity near 6 pN, the force at which the force-extension curves of ssDNA and dsDNA cross. As instrumentation continues to improve, I see no fundamental reason why this assay will not lead to the detection of individual steps of DNAP, as T7 DNAP maintains kinetic activity at high template tensions ($F > 20$ pN).

Both the hairpin-unwinding and the ssDNA-to-dsDNA conversion assays share an important extra benefit: The enzyme under study does not need to be anchored to a surface. Hence, there is no potential perturbation of enzymatic activity associated with surface immobilization, a common concern in surface-coupled assays. These assays also excel at studying molecular motors that are not highly processive. The tug-of-war assay takes time to assemble and is significantly more challenging to implement if the complex is not stable for at least a few minutes.

These benefits come at a cost of increased complexity in interpreting the measured dynamics and energetics, as the applied force no longer directly opposes enzymatic motion. For instance, helicase dynamics can depend on the specific geometry of the unwinding assay (69). Moreover, subtle entropy reductions due to restricted angular orientation can affect the interpretation of DNAP experiments (30).

Processive:

a molecular motor that takes a number of steps before disengaging from its substrate

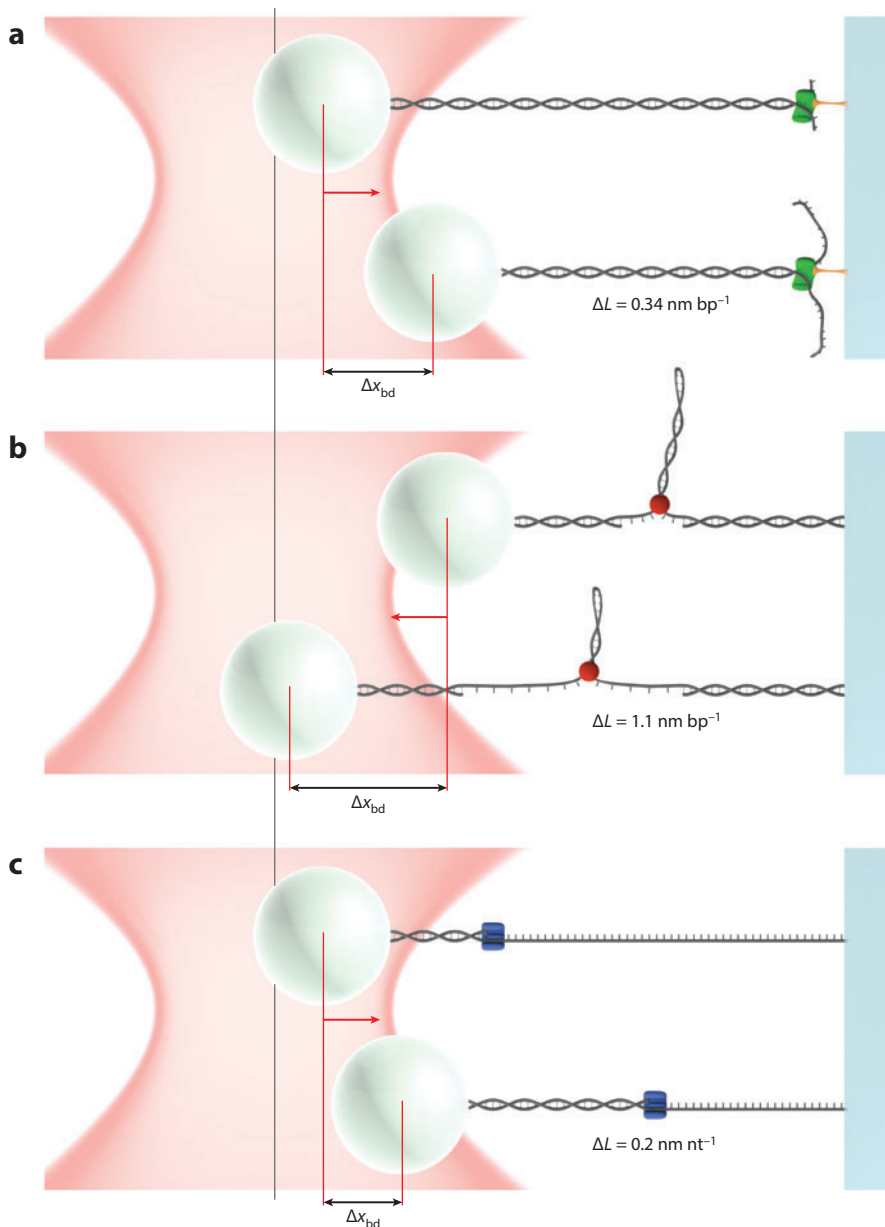
Figure 5

The elasticity of biopolymers affects optical-trapping measurements. (a) A schematic showing a DNA molecule being stretched by an optical trap. For small displacements, the bead moves in the parabolic potential energy (U) well of an optical trap. When the DNA is stretched, both the extension of the DNA (x_{DNA}) and bead position (x_{bd}) change in a coupled fashion depending on their associated stiffness (k_{DNA} and k_{trap}). (b) A schematic showing a dual-trap assay used to stretch DNA. In this setup, the strong trap is operated in the linear regime, allowing for precise measurements of force. Position measurements are done using the weak trap. By pulling the bead out to the maximum in force, small displacements of the bead (Δx_{bd}) do not alter the applied force, F . In other words, the local stiffness of the trap is zero ($k_{\text{trap}} = 0$). In this innovative geometry, the maximum Δx_{bd} is achieved because there is no compliance correction. (c) A trace of 1-Å steps of an isolated bead held in a stiff optical trap ($k_{\text{trap}} = 1.9$ pN nm⁻¹) in which the optics for the trap were surrounded with helium to reduce beam-pointing noise. (d) A record of resolving 1-bp steps by measuring bead motion in the weak trap when the stiff trap is displaced by 3.4 Å. Tension in the DNA was 27 pN. Note the similarity between the signal-to-noise ratio of 1-Å steps of an isolated bead and that of 1-bp steps along DNA. The added complexity and compliance of a bead-DNA-bead system lowers the precision of the assay. Panels b, c, and d adapted with permission from Reference 1.

Dwell time: the time between steps, analysis of which offers a window into enzymatic kinetics beyond just the average rate

Quantifying Steps

Analysis of the steps of individual molecular motors yields a wealth of biologically relevant information; the most obvious of which is the step size. The time between steps, or the dwell time, is also informative. It is linked to the kinetics of the system under study. For an enzyme with one rate-limiting step per mechanical step, the dwell times are exponentially distributed (**Figure 7a,b**). The distributions become more peaked for systems with multiple rate-limiting steps per mechanical translocation (**Figure 7c,d**). Such distributions are described by a gamma distribution, $t^{N-1} \exp(-kt)$, where k is the kinetic rate and N is the number of rate-limiting kinetic



steps per observed mechanical step. Similar analyses have been performed with two unequal kinetic steps (72). For experiments trying to resolve steps along DNA, the rate-limiting kinetic step is typically the arrival of adenosine triphosphate (ATP) or another NTP because the motor is intentionally slowed down to facilitate averaging of Brownian motion.

As the quality and the quantity of stepping data increases, it is important to develop statistically robust ways to detect and analyze steps (13). The best known analysis is the pairwise distance distribution (29). More recently, Kersemakers et al. (42) introduced an algorithm that is widely used, and increasingly sophisticated algorithms continue to be developed (2, 40, 83).

Interestingly, the determination of the effective number of rate-limiting steps is not limited to records in which steps are observed. An extension of earlier work on ion-channel recordings (21) shows that given a sufficiently large number of steps, stochastic fluctuations in dwell times lead to variance in displacement records after a fix time that varies inversely with the number of rate-limiting steps (**Figure 7a**) (72, 81).

A limitation of this class of kinetic analyses is that the individual enzymes need to exhibit the same kinetic parameters. For enzymes that show different kinetic rates for different individual molecules [e.g., RNAP (58)] or for enzymes with kinetic parameters that change slowly or discretely in time [e.g., RecBCD (64)], the analysis should be done on records that exhibit the same kinetic parameters. Simulations are a fruitful way to test the limits of these assumptions.

Detection and Stabilization to One Ångström in Three Dimensions

Decoupling the biological assay from the surface is the most popular method for high-resolution optical-trapping assays. Its usefulness extends beyond molecular motors to include protein folding (78, 98) and DNA-unzipping (19, 70) assays. My lab has focused on an alternative technique, actively stabilizing the surface in 3D with sufficient precision to resolve 1-bp steps. This technique brings Ångström-scale precision to a host of widely used surface-coupled assays. The core concept is similar to that of noise-cancelling headphones: Measure the environmentally induced motion and cancel out that motion in real time.

As a first step, Carter et al. (11) demonstrated stabilization of an optical microscope to 1 Å in 3D over 100 s ($\Delta f = 0.01\text{--}10$ Hz) using forward-scattered light, as is typically done in optical-trapping assays (**Figure 2a**). Two laser beams were critical to this demonstration: One stabilized the sample, and the other independently measured the stability. Researchers need to avoid erroneous conclusions about stability based on the analysis of the in-loop error signal. For instance, in this assay, the feedback loop transfers laser pointing noise to the stage position, resulting in a decrease in stability that is not reported by an in-loop monitor.

Figure 6

Three different assays for measuring molecular motion along DNA lead to three different measured step sizes per 1-bp step of enzymatic motion. (a) The standard tug-of-war assay, in which enzymatic motion is directly opposed by the tension in the DNA, yields a 3.4-Å step size. (b) A hairpin-unwinding assay, which leads to an approximately threefold mechanical amplification of one base pair of unwinding because the length of the taut polymer increases by two nucleotides (nt), and the rise per monomer is greater for ssDNA than for dsDNA. (c) The elasticity of ssDNA differs from that of dsDNA. Thus, the extension at a given F can determine the fraction of ssDNA (as long as the applied load is not near 6 pN, the force at which the extensions of ssDNA and dsDNA are the same). In this assay, the formation of one base pair from one nucleotide results in $\Delta L = 2$ Å. Although they have been drawn in a surface-coupled geometry, all three of these assays can be implemented in dual-trap setups.

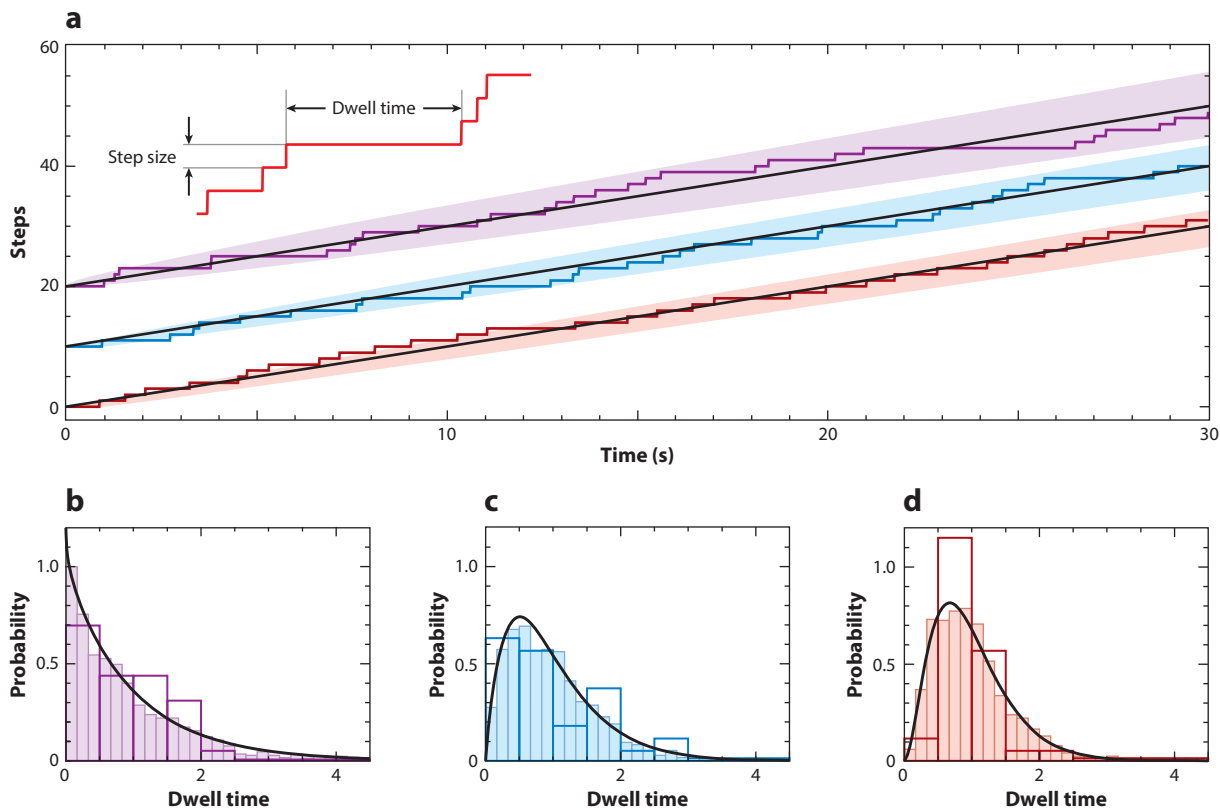


Figure 7

The time between steps yields insight into the kinetics of the enzyme beyond its average translocation rate. (a) Three simulated records of a stochastic stepping enzyme with one (purple), two (blue), and three (red) rate-limiting kinetic steps per observed mechanical step. The rate constant for each simulation was chosen so the average velocity of each record was the same. The dwell time is defined as the time between the steps. Shaded regions represent one standard deviation away from the mean position (black line), determined from 1,000 records for each kinetic condition. (b–d) Histograms of the dwell times calculated from 30 (dark color) or 1,000 (light color) dwell times for one, two, and three rate-limiting steps. Fitting the data to the gamma distribution $t^{N-1} \exp(-kt)$ where k is the kinetic rate and N is the number of rate-limiting kinetic steps per observed step—can be used to determine N for each data set. Fits to the larger data set are shown (black). The resulting determination of N matched the simulated conditions. Best fit values and 95% confidence intervals are 0.96 (0.89, 1.04), 2.03 (1.88, 2.21), and 3.13 (2.88, 3.41) for one, two, and three rate-limiting steps, respectively. However, care must be taken when fitting only a limited number of dwell times.

Carter et al. (10) also demonstrated sample stabilization to 1 Å in 3D over a slightly higher bandwidth ($\Delta f = 0.1$ –50 Hz) using back-scattered light. Back-scattered detection simplifies the mechanical design because highly stable optical components are necessary on only one side of the instrument. Churnside et al. (18) extended this work by improving the rate of feedback such that they were able to achieve sub-Ångström stabilities over 100 s [$\sigma_x = 0.3$ Å; $\sigma_y = 0.2$ Å; $\sigma_z = 0.6$ Å ($\Delta f = 0.01$ –10 Hz)] (Figure 8). More generally, Ångström-scale detection and stabilization with back-scattered light is useful in assays with limited optical access, such as atomic force microscopy (see sidebar, A Laser-Guided Ultrastable Atomic Force Microscope).

Finally, Carter et al. (12) demonstrated 1-bp stability and precision using a traditional surface-coupled optical-trapping assay at a relatively modest F (6 pN) ($\Delta f = 0.03$ –2 Hz). This work

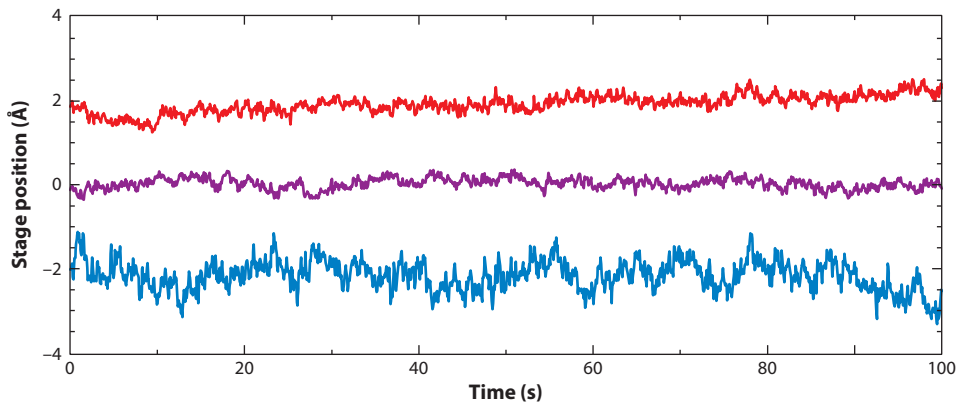


Figure 8

Active stabilization of an optical microscope in three dimensions with back-scattered detection using a field-programmable gate array to achieve a faster feedback rate. Position versus time records, as monitored by an out-of-loop measurement, are shown for x (red), y (purple), and z (blue). These records show sub-Ångström stability over 100 s (0.3, 0.2, and 0.6 Å, for x , y , and z , respectively; $\Delta f = 0.01\text{--}10$ Hz). The larger noise in z is most likely caused by the sensitivity of the z measurements to the total laser intensity. Data smoothed to 10 Hz. Traces displaced for clarity.

A LASER-GUIDED ULTRASTABLE ATOMIC FORCE MICROSCOPE

Atomic force microscopes (AFMs), similar to optical traps, suffer from drift that hinders a range of applications in biology and, more generally, in nanoscience (43). My lab applied the ideas of three-dimensional (3D) optical detection developed for optical traps to AFM. This led to King et al. (43) demonstrating an ultrastable AFM. As in optical traps, two lasers established a local, differential reference frame that is stable to 0.2 Å in 3D (10). We next scattered one laser off the apex of a commercial AFM tip to detect and thereby stabilize its position in 3D. Similarly, we stabilized the sample using the second laser. This merger of optical-trapping technology with AFM led to a tip-sample stability of 4 Å over 80 min, a hundred-fold improvement prior state of the art at ambient conditions. More generally, the 3D position of the AFM tip can now be directly measured, allowing the conjugate variables of force and position to be independently measured.

also discusses the importance of controlling intensity fluctuations of the trapping laser and laser-induced temperature effects that adversely affect high-resolution measurements.

APPLICATIONS TO SELECT MOLECULAR MOTORS

Pauses in Motion Are as Informative as Steps

The music is not in the notes, but in the silence between.
—Attributed to Mozart

In music, the pauses between notes can be as poignant as the notes themselves. For DNA-based molecular motors, in general, and for RNAP, in particular, the detection of pauses in motion is having a much larger biological impact than is the resolution of 1-bp steps (24, 28, 35, 47, 58, 99,

100). Pauses in RNAP motion were detected in traditional gel assays and in early trapping studies (91, 96). Pauses were initially a hindrance to determining pause-free velocities for $F-v$ analysis (91). However, the advent of high-stability optical traps enabled mechanistic insight into the dynamics of an individual RNAP relative to the DNA during a pause (58, 75). Different duration pauses were associated with a different level of motion of the RNAP relative to the template (47). For instance, longer backtracking pauses of *Escherichia coli* RNAP are associated with ~ 5 bp of motion (75), whereas ubiquitous pauses are not (58). These ubiquitous pauses are sufficiently short that they were not detected using ensemble assays. One particularly interesting class of pauses are sequence-specific regulatory pauses, which may facilitate cotranscriptional folding of the RNA (44).

The primary measurement problem in optical-trapping studies of sequence-dependent pausing is an issue not of precision but of accuracy. The radius of the bead (r_{bd}) is used in determining L . Thus, variations in r_{bd} lead to variations in L , making accurate correlation between the value of L and a specific sequence challenging. Beads with 2% variation in r_{bd} are considered very uniform in size. But, for a r_{bd} of 300 nm, this uncertainty leads to an 18-bp uncertainty along the DNA (63). This effect is magnified in a dual-trap assay using two beads. In a surface-coupled assay, Perkins et al. (63) demonstrated a direct correlation between a strong sequence-dependent pause of lambda exonuclease and a specific sequence; this accuracy required subtracting out the average stage drift during the experiment, aligning traces via a dominant pause, and averaging over many beads. Different sequences had different pause strengths (as determined from the probability of pausing and the pause duration). Notably, these single-molecule studies determined a myriad of sequence-dependent pauses that were undetected using the traditional gel analysis (63).

Herbert et al. (36) introduced a more useful assay that requires precision instead of accuracy. Their insight was to repeat the same sequence multiple times within the DNA molecule (**Figure 9a**). The resulting records showed repetitive pauses (**Figure 9b**) for which the analysis (**Figure 9c**) required only a measurement of the relative distance. Computational alignment and adjustment in this case leads to 1-bp precision. Although repetitive sequences are challenging to make, such substrates hold great promise for increasing precision and statistics in single-molecule studies. The same individual enzyme interacts with the same sequence multiple times, enabling variations in the individual enzyme's response to be probed.

Mechanistic Insight from Improved Spatiotemporal Resolution

While new insights into the kinetic pathway of RNAP are derived from analyzing pauses (99, 100), step-size determination is providing exciting mechanistic conclusions in an increasing number of other systems. Moreover, improvements in spatiotemporal resolution to sub-base pair levels are leading to nonintuitive models, particularly for helicases (16) and DNA packaging into bacteriophage capsids (52).

Optical-tapping studies of the RNA helicase NS3 showed large steps of 11 ± 3 bp, equal to a 22-nt increase in L in the hairpin-unwinding assay (26). By slowing down the stepping of NS3, Dumont et al. (26) observed smaller substeps (3.6 ± 1.3 bp) within these large steps (**Figure 10a**). The precision of this assay was limited to ~ 2 bp, most likely because of the mechanical motion of the micropipette used in this assay. The combination of a large step with smaller steps suggested an inchworming mechanism. Subsequent single-molecule FRET studies confirmed a 3-bp step (57). Interestingly, dwell time analysis showed three rate-limiting steps per observed step, consistent with three ATPs binding per 3-bp step. The authors put forward an ATP-driven internal conformational change not probed by the position of the FRET dye pair. Improvements in

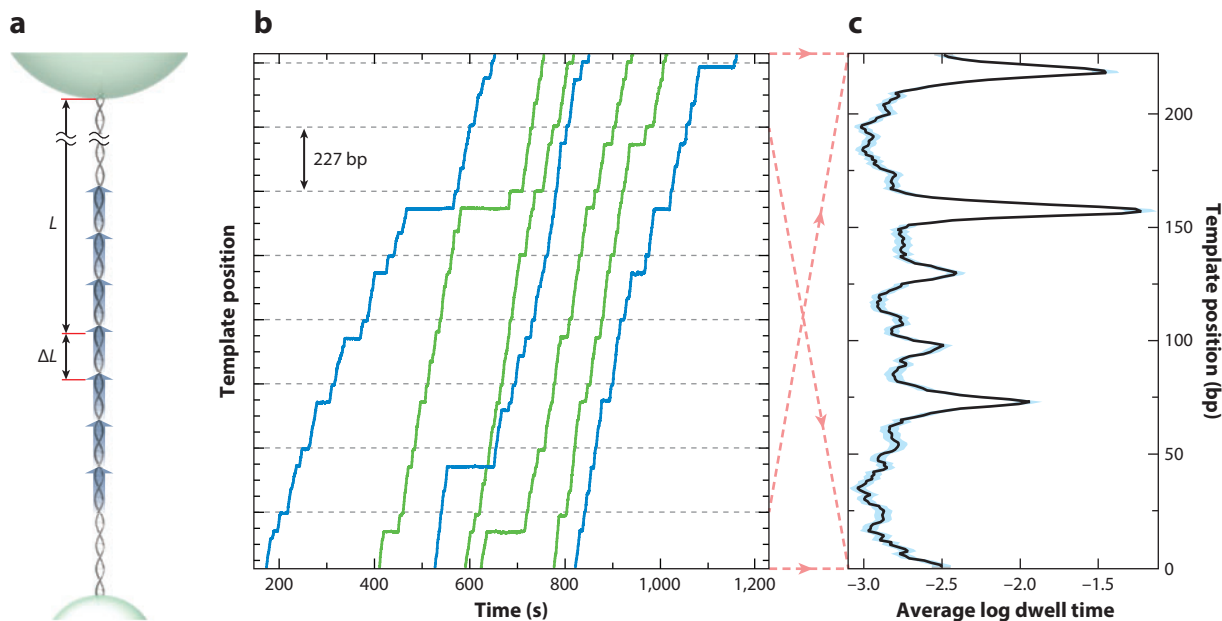


Figure 9

A repetitive DNA template facilitates the analysis of sequence-dependent pauses. (a) Schematic of a DNA template for RNA polymerase (RNAP) that contains multiple repeats of the same sequence. This construct simplified the connection of enzymatic dynamics with the underlying DNA sequence because correlating the absolute location on the DNA template (L) is much harder than measuring precise changes in L (ΔL). This difficulty is primarily caused by small variations in the bead radii. (b) Traces of RNAP motion along this template show sequence-dependent pausing. Pause-inducing sequences are located every 227 bp (gray dashed lines), but these do not produce the strongest pauses in the repeated region. (c) A histogram of dwell time versus template position assembled from each of the repetitive segments highlights strong sequence-specific pauses. Figure adapted with permission from Reference 36.

stability afforded by the dual-beam assay (1), as well as improvements in spatiotemporal precision (17, 53), allowed Cheng et al. (16) to resolve these anticipated 1-bp steps of NS3 within the larger 11-bp steps (Figure 10b, left panel). The real mechanistic surprise was the presence of 1.5-bp steps, or, more precisely, a 3-nt increase in L (Figure 10b, right panel). The authors interpreted these steps as an unwinding of the RNA duplex by one base pair during which the helicase released three nucleotides; the extra nucleotide was sequestered by the NS3 during a previous unwinding cycle.

The importance of being able to confidently resolve half-integer step sizes is not limited to helicases; it extends to the portal protein of bacteriophage $\phi 29$. Similar to NS3, this protein showed a large step size (10 bp). Given its pentameric structure, the most parsimonious explanation would be a series of five 2-bp steps. However, in a remarkably precise experiment, Moffitt et al. (52) showed that the dwell time histograms of these 10-bp steps were consistent with four rate-limiting steps, a conclusion confirmed by measuring sets of four 2.5-bp steps (Figure 1d).

These new mechanistic insights, and others, motivate the ongoing need to improve the spatiotemporal precision of optical traps. Most high-resolution studies are done at high force and subsaturating levels of NTPs. High force makes the whole system stiffer, decreasing the magnitude of Brownian motion and enabling more rapid averaging of the remaining motion. Both high force and low ATP lead to slower steps. Ideally, these high-resolution studies will be extended to less perturbative conditions of lower force and saturating levels of NTPs.

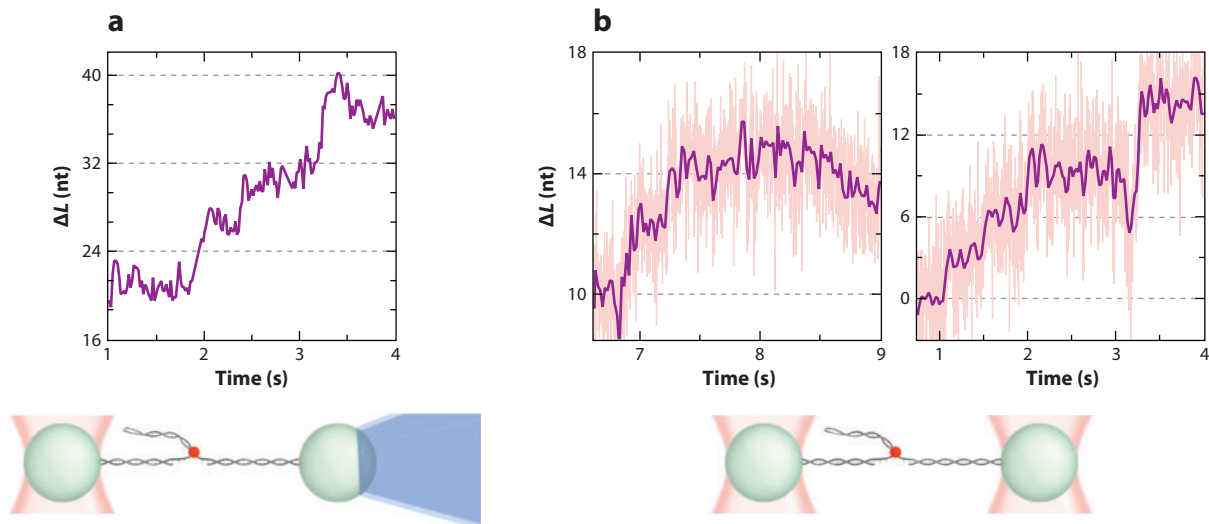


Figure 10

Stepping of the RNA helicase NS3 studied using the hairpin-unwinding assay. (a) Record of enzymatic motion measured using a combination of an optical trap and a micropipette. This surface-coupled assay revealed discrete steps, monitored by the increase in stretched DNA and measured in nucleotides (nt) [2 nt are equal to 1 base pair (bp) of unwinding]. Adapted with permission from Reference 26. (b) Enzymatic motion measured using a dual-trap assay improves mechanical stability. (left) Record showing 2-nt increases in contour length, L , which are consistent with 1-bp steps. (right) Record showing 3-nt increases in L , which are consistent with 1-bp steps and the release of 1 nt held by the enzyme. Panel adapted with permission from Reference 16.

EMERGING TECHNICAL ADVANCES AND NEXT STEPS

Currently, assays using optical traps with Ångström-scale precision are leading to important biological insights. Their utility can be expanded by further technical enhancements, including improved spatiotemporal resolution, improved stability, and integration with other single-molecule techniques.

Improved spatiotemporal resolution will facilitate step detection of molecular motors operating at or near saturating levels of NTPs. Two fruitful avenues of research are better beads and stiffer handles. Better beads would be smaller, enabling faster averaging of Brownian motion, and would have an increased k_{trap} relative to typical beads (polystyrene or glass) at a fixed laser power. This increased k_{trap} is necessary because significantly smaller standard beads cannot exert the 10–20 pN needed for high-resolution studies at biologically useful conditions. Gold nanoparticles initially looked promising (34), but they suffered from too much heating for these assays (73). More recently, Jannasch et al. (39) made titania core-shell microspheres that were 1 μm in diameter and that exhibited a threefold increase in k_{trap} .

Stiffer handles—the total compliance between the two attachment points—make the whole system stiffer, increasing the temporal resolution. One possibility is using very short linkers between the beads. Although this possibility is attractive, one quickly runs into crosstalk and even hopping of the bead between traps in a dual-trap setup (51), unless rather large beads are used (70), which decreases the temporal resolution as a result of hydrodynamic drag. In most high-precision stepping assays, most of the DNA is not traversed during the experiment. Rather, the DNA is being used to space the beads far enough apart to avoid crosstalk. Kauert et al. (41) provide evidence for an interesting idea: using DNA origami to make stiff handles.

Resolving an extended series of steps with 1-bp precision remains a difficult problem. The current standard in the field is to show 6–8 records of 8–10 steps. The skeleton in the closet is that large sections of the data do not show clearly resolved steps. Improving the stability of the instrument and the mechanical linkages in the assay should enable high-precision analysis of an increased fraction of each record. Moreover, these enhancements will also increase the confidence in interpretations of data showing non-step-like protein motion that arises from changes in molecular conformation. Prospects for improved low-frequency stability include more compact optical paths with increased common-mode elements (10), lock-in detection (84), and FPGA-based control for more sophisticated real-time feedback (18, 90).

Mechanical measurements offer just one way to probe a molecule. A more complete picture is generated by combining multiple techniques. The combination of high-resolution optical traps with single-molecule fluorescence (22, 76) in general, and with single-molecule FRET (38, 46) in particular, is an increasingly important tool. A critical technical advance is interlacing of the trapping beam with the fluorescence excitation to minimize photobleaching (7). The successful three-way integration of dual-beam traps, single-molecule fluorescence, and microfluidics is proving fruitful (9). The challenge going forward is to achieve 1-bp stability in a microfluidic device.

SUMMARY

High-resolution optical-trapping experiments are technically demanding, but they enable a tremendous amount of science. At a more personal level, it is satisfying to watch individual proteins move or unfold in real time with Ångström-scale precision, the scale of individual atomic bonds. The technical underpinning of this impressive feat is an optically based reference frame. The ultimate stability is limited by the differential pointing stability of two laser beams, which is currently ~ 0.2 Å (10). Understanding the compliance of biological molecules and moderating its impact has been an important factor in advancing high-resolution studies. Future improvements in both areas will be important as multiprotein assemblies such as the replisome (87) are studied.

For brevity, this review has focused on a particular set of applications, DNA-based motor proteins, but the powerful advancement in instrumentation described herein can benefit large areas of biophysical research. For instance, broad classes of enzymatic activity lead to conformational changes. Such Ångström-scale motion is now detectable with an optical trap; this work is conceptually similar to earlier work using an AFM to study the conformational dynamics of lysozyme (68) but has the added assurance of long-term instrumental stability. This and many other exciting applications will be aided by increasing the reliability and throughput of optical traps with Ångström-scale precision and stability.

SUMMARY POINTS

1. Optical traps can resolve molecular motion in real-time with 1-Ångström precision.
2. Long-term stability is enabled by an optically based reference frame established by two lasers with very low differential pointing stability.
3. Additional elasticity of the biological assay degrades instrumental precision.
4. Advances in optical-trapping geometry, assays, and templates improve the precision and range of systems that can be studied.
5. Pauses in motion can be as informative as step-size determination.

DISCLOSURE STATEMENT

The author is a coinventor on two US patents related to Ångström-scale stabilization. These patents are assigned to the US government.

ACKNOWLEDGMENTS

I would like to thank Brad Baxley, George Emanuel, and Matt Bull for figure preparation. I am grateful to Keir Neuman, Joshua Shaevitz, and the whole Perkins group for critical reading of the manuscript and to members of the single-molecule biophysics community for sharing their data. This work was supported by the Burroughs Wellcome Fund, the National Science Foundation (grant numbers Phy-0404286, DBI-0923544, and PHY-1125844), and the National Institute of Standards and Technology (NIST). T.T.P. is a staff member of the Quantum Physics Division of NIST.

LITERATURE CITED

1. Resolves 1–base pair steps of RNA polymerase along DNA.

7. Significantly improves the combination of optical traps and single-molecule fluorescence by high-frequency interlacing of the trapping and the illumination lasers.

1. Abbondanzieri EA, Greenleaf WJ, Shaevitz JW, Landick R, Block SM. 2005. Direct observation of base-pair stepping by RNA polymerase. *Nature* 438:460–65
2. Arunajadai SG, Cheng W. 2013. Step detection in single-molecule real time trajectories embedded in correlated noise. *PLoS ONE* 8:e59279
3. Aubin-Tam ME, Olivares AO, Sauer RT, Baker TA, Lang MJ. 2011. Single-molecule protein unfolding and translocation by an ATP-fueled proteolytic machine. *Cell* 145:257–67
4. Bai L, Santangelo TJ, Wang MD. 2006. Single-molecule analysis of RNA polymerase transcription. *Annu. Rev. Biophys. Biomol. Struct.* 35:343–60
5. Berg JM, Tymoczko JL, Stryer L. 2010. *Biochemistry*. New York: W. H. Freeman
6. Bianco PR, Brewer LR, Corzett M, Balhorn R, Yeh Y, et al. 2001. Processive translocation and DNA unwinding by individual RecBCD enzyme molecules. *Nature* 409:374–78
7. Brau RR, Tarsa PB, Ferrer JM, Lee P, Lang MJ. 2006. Interlaced optical force-fluorescence measurements for single molecule biophysics. *Biophys. J.* 91:1069–77
8. Bustamante C, Marko JF, Siggia ED, Smith SB. 1994. Entropic elasticity of λ -phage DNA. *Science* 265:1599–600
9. Candelli A, Wuite GJL, Peterman EJG. 2011. Combining optical trapping, fluorescence microscopy and micro-fluidics for single molecule studies of DNA-protein interactions. *Phys. Chem. Chem. Phys.* 13:7263–72
10. Carter AR, King GM, Perkins TT. 2007. Back-scattered detection provides atomic-scale localization precision, stability, and registration in 3D. *Opt. Express* 15:13434–45
11. Carter AR, King GM, Ulrich TA, Halsey W, Alchenberger D, Perkins TT. 2007. Stabilization of an optical microscope to 0.1 nm in three dimensions. *Appl. Opt.* 46:421–27
12. Carter AR, Seol Y, Perkins TT. 2009. Precision surface-coupled optical-trapping assays with 1 base-pair resolution. *Biophys. J.* 96:2926–34
13. Carter BC, Vershinin M, Gross SP. 2008. A comparison of step-detection methods: How well can you do? *Biophys. J.* 94:306–19
14. Chemla YR. 2010. Revealing the base pair stepping dynamics of nucleic acid motor proteins with optical traps. *Phys. Chem. Chem. Phys.* 12:3080–95
15. Chemla YR, Smith DE. 2012. Single-molecule studies of viral DNA packaging. *Adv. Exp. Med. Biol.* 726:549–84
16. Cheng W, Arunajadai SG, Moffitt JR, Tinoco IJ, Bustamante C. 2011. Single-base pair unwinding and asynchronous RNA release by the hepatitis C virus NS3 helicase. *Science* 333:1746–49
17. Cheng W, Hou X, Ye F. 2010. Use of tapered amplifier diode laser for biological-friendly high-resolution optical trapping. *Opt. Lett.* 35:2988–90

18. Churnside AB, King GM, Carter AR, Perkins TT. 2008. Improved performance of an ultrastable measurement platform using a field-programmable gate array for real-time deterministic control. *Proc. SPIE* 7042:704205
19. Cisse I, Mangeol P, Bockelmann U. 2011. DNA unzipping and force measurements with a dual optical trap. *Methods Mol. Biol.* 783:45–61
20. Cluzel P, Lebrun A, Heller C, Lavery R, Viovy JL, et al. 1996. DNA: an extensible molecule. *Science* 271:792–94
21. Colquhoun D. 1971. *Lectures on Biostatistics; an Introduction to Statistics with Applications in Biology and Medicine*. Oxford: Clarendon
22. Comstock MJ, Ha T, Chemla YR. 2011. Ultrahigh-resolution optical trap with single-fluorophore sensitivity. *Nat. Methods* 8:335–40
23. Czerwinski F, Richardson AC, Oddershede LB. 2009. Quantifying noise in optical tweezers by Allan variance. *Opt. Express* 17:13255–69
24. Dalal RV, Larson MH, Neuman KC, Gelles J, Landick R, Block SM. 2006. Pulling on the nascent RNA during transcription does not alter kinetics of elongation or ubiquitous pausing. *Mol. Cell* 23:231–39
25. Denk W, Webb WW. 1990. Optical measurement of picometer displacements of transparent microscopic objects. *Appl. Opt.* 29:2382–91
26. Dumont S, Cheng W, Serebrov V, Beran RK, Tinoco JJ, et al. 2006. RNA translocation and unwinding mechanism of HCV NS3 helicase and its coordination by ATP. *Nature* 439:105–8
27. Finer JT, Simmons RM, Spudich JA. 1994. Single myosin molecule mechanics: piconewton forces and nanometre steps. *Nature* 368:113–19
28. Galbur EA, Grill SW, Wiedmann A, Lubkowska L, Choy J, et al. 2007. Backtracking determines the force sensitivity of RNAP II in a factor-dependent manner. *Nature* 446:820–23
29. Gelles J, Schnapp BJ, Sheetz MP. 1988. Tracking kinesin-driven movements with nanometre-scale precision. *Nature* 331:450–53
30. Goel A, Astumian RD, Herschbach D. 2003. Tuning and switching a DNA polymerase motor with mechanical tension. *Proc. Natl. Acad. Sci. USA* 100:9699–704
31. Greenleaf WJ, Woodside MT, Abbondanzieri EA, Block SM. 2005. **Passive all-optical force clamp for high-resolution laser trapping.** *Phys. Rev. Lett.* 95:208102
32. Greenleaf WJ, Woodside MT, Block SM. 2007. High-resolution, single-molecule measurements of biomolecular motion. *Annu. Rev. Biophys. Biomol. Struct.* 36:171–90
33. Hagerman PJ. 1988. Flexibility of DNA. *Annu. Rev. Biophys. Biophys. Chem.* 17:265–86
34. Hansen PM, Bhatia VK, Harrit N, Oddershede L. 2005. Expanding the optical trapping range of gold nanoparticles. *Nano Lett.* 5:1937–42
35. Herbert KM, Greenleaf WJ, Block SM. 2008. Single-molecule studies of RNA polymerase: motoring along. *Annu. Rev. Biochem.* 77:149–76
36. Herbert KM, La Porta A, Wong BJ, Mooney RA, Neuman KC, et al. 2006. Sequence-resolved detection of pausing by single RNA polymerase molecules. *Cell* 125:1083–94
37. Hoffmann A, Neupane K, Woodside MT. 2013. Single-molecule assays for investigating protein misfolding and aggregation. *Phys. Chem. Chem. Phys.* 15:7934–48
38. Hohng S, Zhou R, Nahas MK, Yu J, Schulten K, et al. 2007. Fluorescence-force spectroscopy maps two-dimensional reaction landscape of the Holliday junction. *Science* 318:279–83
39. Jannasch A, Demirors AF, van Oostrum PDJ, van Blaaderen A, Schaffer E. 2012. Nanonewton optical force trap employing anti-reflection coated, high-refractive-index titania microspheres. *Nat. Photonics* 6:469–73
40. Kalafut B, Visscher K. 2008. An objective, model-independent method for detection of non-uniform steps in noisy signals. *Comput. Phys. Commun.* 179:716–23
41. Kauert DJ, Kurth T, Liedl T, Seidel R. 2011. Direct mechanical measurements reveal the material properties of three-dimensional DNA origami. *Nano Lett.* 11:5558–63
42. Kerssemakers JW, Munteanu EL, Laan L, Noetzel TL, Janson ME, Dogterom M. 2006. Assembly dynamics of microtubules at molecular resolution. *Nature* 442:709–12

31. Demonstrates a new trapping geometry, the passive force clamp, that provides for improved force control.

43. Extends optical detection techniques of optical traps to enable an ultrastable atomic force microscope.

52. Demonstrates a pentameric molecular motor making a rapid series of four 2.5-base pair steps.

43. King GM, Carter AR, Churnside AB, Eberle LS, Perkins TT. 2009. Ultrastable atomic force microscopy: atomic-scale lateral stability and registration in ambient condition. *Nano Lett.* 9:1451–56
44. Landick R. 2006. The regulatory roles and mechanism of transcriptional pausing. *Biochem. Soc. Trans.* 34:1062–66
45. Lang MJ, Block SM. 2003. Resource letter: LBOT-1: laser-based optical tweezers. *Am. J. Phys.* 71:201–15
46. Lang MJ, Fordyce PM, Engh AM, Neuman KC, Block SM. 2004. Simultaneous, coincident optical trapping and single-molecule fluorescence. *Nat. Methods* 1:133–39
47. Larson MH, Landick R, Block SM. 2011. Single-molecule studies of RNA polymerase: one singular sensation, every little step it takes. *Mol. Cell* 41:249–62
48. Liphardt J, Onoa B, Smith SB, Tinoco IJ, Bustamante C. 2001. Reversible unfolding of single RNA molecules by mechanical force. *Science* 292:733–37
49. Maillard RA, Chistol G, Sen M, Righini M, Tan JY, et al. 2011. ClpX(P) generates mechanical force to unfold and translocate its protein substrates. *Cell* 145:459–69
50. Marko JF, Siggia ED. 1995. Stretching DNA. *Macromolecules* 28:8759–70
51. McCann LI, Dykman M, Golding B. 1999. Thermally activated transitions in a bistable three-dimensional optical trap. *Nature* 402:785–87
52. Moffitt JR, Chemla YR, Aathavan K, Grimes S, Jardine PJ, et al. 2009. Intersubunit coordination in a homomeric ring ATPase. *Nature* 457:446–50
53. Moffitt JR, Chemla YR, Izhaky D, Bustamante C. 2006. Differential detection of dual traps improves the spatial resolution of optical tweezers. *Proc. Natl. Acad. Sci. USA* 103:9006–11
54. Moffitt JR, Chemla YR, Smith SB, Bustamante C. 2008. Recent advances in optical tweezers. *Annu. Rev. Biochem.* 77:205–28
55. Molloy JE, Burns JE, Kendrick-Jones J, Tregear RT, White DCS. 1995. Movement and force produced by a single myosin head. *Nature* 378:209–12
56. Morin JA, Cao FJ, Lazaro JM, Arias-Gonzalez JR, Valpuesta JM, et al. 2012. Active DNA unwinding dynamics during processive DNA replication. *Proc. Natl. Acad. Sci. USA* 109:8115–20
57. Myong S, Bruno MM, Pyle AM, Ha T. 2007. Spring-loaded mechanism of DNA unwinding by hepatitis C virus NS3 helicase. *Science* 317:513–16
58. Neuman KC, Abbondanzieri EA, Landick R, Gelles J, Block SM. 2003. Ubiquitous transcriptional pausing is independent of RNA polymerase backtracking. *Cell* 115:437–47
59. Neuman KC, Block SM. 2004. Optical trapping. *Rev. Sci. Instrum.* 75:2787–809
60. Neuman KC, Nagy A. 2008. Single-molecule force spectroscopy: optical tweezers, magnetic tweezers and atomic force microscopy. *Nat. Methods* 5:491–505
61. Nugent-Glandorf L, Perkins TT. 2004. Measuring 0.1-nm motion in 1 ms in an optical microscope with differential back-focal-plane detection. *Opt. Lett.* 29:2611–13
62. Perkins TT. 2009. Optical traps for single molecule biophysics: a primer. *Laser Photonics Rev.* 3:203–20
63. Perkins TT, Dalal RV, Mitsis PG, Block SM. 2003. Sequence-dependent pausing of single lambda exonuclease molecules. *Science* 301:1914–18
64. Perkins TT, Li HW, Dalal RV, Gelles J, Block SM. 2004. Forward and reverse motion of single RecBCD molecules on DNA. *Biophys. J.* 86:1640–48
65. Perkins TT, Quake SR, Smith DE, Chu S. 1994. Relaxation of a single DNA molecule observed by optical microscopy. *Science* 264:822–26
66. Perkins TT, Smith DE, Chu S. 1994. Direct observation of tube-like motion of a single polymer chain. *Science* 264:819–22
67. Quake SR, Babcock H, Chu S. 1997. The dynamics of partially extended single molecules of DNA. *Nature* 388:151–54
68. Radmacher M, Fritz M, Hansma HG, Hansma PK. 1994. Direct observation of enzyme activity with the atomic force microscope. *Science* 265:1577–79
69. Ribeck N, Kaplan DL, Bruck I, Saleh OA. 2010. DnaB helicase activity is modulated by DNA geometry and force. *Biophys. J.* 99:2170–79

70. Ribezzi-Crivellari M, Huguët JM, Ritort F. 2013. Counter-propagating dual-trap optical tweezers based on linear momentum conservation. *Rev. Sci. Instrum.* 84:043104
71. Roy R, Hohng S, Ha T. 2008. A practical guide to single-molecule FRET. *Nat. Methods* 5:507–16
72. Schnitzer MJ, Block SM. 1997. Kinesin hydrolyses one ATP per 8-nm step. *Nature* 388:386–90
73. Seol Y, Carpenter AE, Perkins TT. 2006. Gold nanoparticles: enhanced optical trapping and sensitivity coupled with significant heating. *Opt. Lett.* 31:2429–31
74. Seol Y, Li J, Nelson PC, Perkins TT, Betterton MD. 2007. Elasticity of short DNA molecules: theory and experiment for contour lengths of 0.6–7 μm . *Biophys. J.* 93:4360–73
75. **Shaevitz JW, Abbondanzieri EA, Landick R, Block SM. 2003. Backtracking by single RNA polymerase molecules observed at near-base-pair resolution. *Nature* 426:684–87**
76. Sirinakis G, Ren Y, Gao Y, Xi Z, Zhang Y. 2012. Combined versatile high-resolution optical tweezers and single-molecule fluorescence microscopy. *Rev. Sci. Instrum.* 83:093708
77. Smith SB, Cui Y, Bustamante C. 1996. Overstretching of B-DNA: the elastic response of individual double-stranded and single-stranded DNA molecules. *Science* 271:795–99
78. **Stigler J, Ziegler F, Gieseke A, Gebhardt JCM, Rief M. 2011. The complex folding network of single calmodulin molecules. *Science* 334:512–16**
79. Sullivan DB, Allan DW, Howe DA, Walls EL, eds. 1990. *Characterization of Clocks and Oscillators*. Washington, DC: USGPO
80. Svoboda K, Block SM. 1994. Biological applications of optical forces. *Annu. Rev. Biophys. Biomol. Struct.* 23:247–85
81. Svoboda K, Block SM. 1994. Force and velocity measured for single kinesin molecules. *Cell* 77:773–84
82. Svoboda K, Schmidt CF, Schnapp BJ, Block SM. 1993. Direct observation of kinesin stepping by optical trapping interferometry. *Nature* 365:721–27
83. Syed S, Müllner FE, Selvin PR, Sigworth FJ. 2010. Improved hidden Markov models for molecular motors, Part 2: extensions and application to experimental data. *Biophys. J.* 99:3696–703
84. Taylor MA, Knittel J, Bowen WP. 2013. Optical lock-in particle tracking in optical tweezers. *Opt. Express* 21:8018–24
85. Tinoco I, Chen G, Qu X. 2010. RNA reactions one molecule at a time. *Cold Spring Harb. Perspect. Biol.* 2:a003624
86. van Mameren J, Wuite GJ, Heller I. 2011. Introduction to optical tweezers: background, system designs, and commercial solutions. *Methods Mol. Biol.* 783:1–20
87. van Oijen AM, Loparo JJ. 2010. Single-molecule studies of the replisome. *Annu. Rev. Biophys.* 39:429–48
88. Visscher K, Gross SP, Block SM. 1996. Construction of multiple-beam optical traps with nanometer-resolution position sensing. *IEEE J. Sel. Top. Quant. Electron.* 2:1066–76
89. **Visscher K, Schnitzer MJ, Block SM. 1999. Single kinesin molecules studied with a molecular force clamp. *Nature* 400:184–89**
90. Wallin AE, Ojala H, Haeggstrom E, Tuma R. 2008. Stiffer optical tweezers through real-time feedback control. *Appl. Phys. Lett.* 92:224104
91. Wang MD, Schnitzer MJ, Yin H, Landick R, Gelles J, Block SM. 1998. Force and velocity measured for single molecules of RNA polymerase. *Science* 282:902–7
92. Wang MD, Yin H, Landick R, Gelles J, Block SM. 1997. Stretching DNA with optical tweezers. *Biophys. J.* 72:1335–46
93. **Wen JD, Lancaster L, Hodges C, Zeri AC, Yoshimura SH, et al. 2008. Following translation by single ribosomes one codon at a time. *Nature* 452:598–603**
94. Wuite GJL, Smith SB, Young M, Keller D, Bustamante C. 2000. Single-molecule studies of the effect of template tension on T7 DNA polymerase activity. *Nature* 404:103–6
95. Yin H, Landick R, Gelles J. 1994. Tethered particle motion method for studying transcript elongation by a single RNA polymerase molecule. *Biophys. J.* 67:2468–78
96. Yin H, Wang MD, Svoboda K, Landick R, Block SM, Gelles J. 1995. Transcription against an applied force. *Science* 270:1653–57
97. Yodh JG, Schlierf M, Ha T. 2010. Insight into helicase mechanism and function revealed through single-molecule approaches. *Q. Rev. Biophys.* 43:185–217

75. Introduces the dual-trap assay for studying RNA polymerase with significantly enhanced long-term stability.

78. Demonstrates the utility of a dual-beam optical trap for providing a highly detailed picture of a single calmodulin molecule folding and unfolding.

89. Demonstrates the application of a force clamp to enable high-resolution studies of single molecules.

93. Observes 1-codon steps of an individual ribosome along RNA.

98. Yu H, Liu X, Neupane K, Gupta AN, Brigley AM, et al. 2012. Direct observation of multiple misfolding pathways in a single prion protein molecule. *Proc. Natl. Acad. Sci. USA* 109:5283–88
99. Zhou J, Ha KS, La Porta A, Landick R, Block SM. 2011. Applied force provides insight into transcriptional pausing and its modulation by transcription factor NusA. *Mol. Cell* 44:635–46
100. Zhou J, Schweikhard V, Block SM. 2013. Single-molecule studies of RNAPII elongation. *Biochim. Biophys. Acta* 1829:29–38



Contents

Fun and Games in Berkeley: The Early Years (1956–2013) <i>Ignacio Tinoco Jr.</i>	1
Reconstructing Folding Energy Landscapes by Single-Molecule Force Spectroscopy <i>Michael T. Woodside and Steven M. Block</i>	19
Mechanisms Underlying Nucleosome Positioning In Vivo <i>Amanda L. Hughes and Oliver J. Rando</i>	41
Microfluidics Expanding the Frontiers of Microbial Ecology <i>Roberto Rusconi, Melissa Garren, and Roman Stocker</i>	65
Bacterial Multidrug Efflux Transporters <i>Jared A. Delmar, Chih-Chia Su, and Edward W. Yu</i>	93
Mechanisms of Cellular Proteostasis: Insights from Single-Molecule Approaches <i>Carlos J. Bustamante, Christian M. Kaiser, Rodrigo A. Maillard, Daniel H. Goldman, and Christian A.M. Wilson</i>	119
Biophysical Challenges to Axonal Transport: Motor-Cargo Deficiencies and Neurodegeneration <i>Sandra E. Encalada and Lawrence S.B. Goldstein</i>	141
Live Cell NMR <i>Darón I. Freedberg and Philipp Selenko</i>	171
Structural Bioinformatics of the Interactome <i>Donald Petrey and Barry Honig</i>	193
Bringing Bioelectricity to Light <i>Adam E. Cohen and Veena Venkatachalam</i>	211
Energetics of Membrane Protein Folding <i>Karen G. Fleming</i>	233
The Fanconi Anemia DNA Repair Pathway: Structural and Functional Insights into a Complex Disorder <i>Helen Walden and Andrew J. Deans</i>	257

Ångström-Precision Optical Traps and Applications <i>Thomas T. Perkins</i>	279
Photocontrollable Fluorescent Proteins for Superresolution Imaging <i>Daria M. Shcherbakova, Prabuddha Sengupta, Jennifer Lippincott-Schwartz, and Vladislav V. Verkhusha</i>	303
Itch Mechanisms and Circuits <i>Liang Han and Xinzhong Dong</i>	331
Structural and Functional Insights to Ubiquitin-Like Protein Conjugation <i>Frederick C. Streib Jr. and Christopher D. Lima</i>	357
Fidelity of Cotranslational Protein Targeting by the Signal Recognition Particle <i>Xin Zhang and Shu-ou Shan</i>	381
Metals in Protein–Protein Interfaces <i>Woon Ju Song, Pamela A. Sontz, Xavier I. Ambroggio, and F. Akif Tezcan</i>	409
Computational Analysis of Conserved RNA Secondary Structure in Transcriptomes and Genomes <i>Sean R. Eddy</i>	433

Index

Cumulative Index of Contributing Authors, Volumes 39–43	457
---	-----

Errata

An online log of corrections to *Annual Review of Biophysics* articles may be found at
<http://www.annualreviews.org/errata/biophys>



ANNUAL REVIEWS

It's about time. Your time. It's time well spent.

New From Annual Reviews:

Annual Review of Statistics and Its Application

Volume 1 • Online January 2014 • <http://statistics.annualreviews.org>

Editor: **Stephen E. Fienberg**, *Carnegie Mellon University*

Associate Editors: **Nancy Reid**, *University of Toronto*

Stephen M. Stigler, *University of Chicago*

The *Annual Review of Statistics and Its Application* aims to inform statisticians and quantitative methodologists, as well as all scientists and users of statistics about major methodological advances and the computational tools that allow for their implementation. It will include developments in the field of statistics, including theoretical statistical underpinnings of new methodology, as well as developments in specific application domains such as biostatistics and bioinformatics, economics, machine learning, psychology, sociology, and aspects of the physical sciences.

Complimentary online access to the first volume will be available until January 2015.

TABLE OF CONTENTS:

- *What Is Statistics?* Stephen E. Fienberg
- *A Systematic Statistical Approach to Evaluating Evidence from Observational Studies*, David Madigan, Paul E. Stang, Jesse A. Berlin, Martijn Schuemie, J. Marc Overhage, Marc A. Suchard, Bill Dumouchel, Abraham G. Hartzema, Patrick B. Ryan
- *The Role of Statistics in the Discovery of a Higgs Boson*, David A. van Dyk
- *Brain Imaging Analysis*, F. DuBois Bowman
- *Statistics and Climate*, Peter Guttorp
- *Climate Simulators and Climate Projections*, Jonathan Rougier, Michael Goldstein
- *Probabilistic Forecasting*, Tilmann Gneiting, Matthias Katzfuss
- *Bayesian Computational Tools*, Christian P. Robert
- *Bayesian Computation Via Markov Chain Monte Carlo*, Radu V. Craiu, Jeffrey S. Rosenthal
- *Build, Compute, Critique, Repeat: Data Analysis with Latent Variable Models*, David M. Blei
- *Structured Regularizers for High-Dimensional Problems: Statistical and Computational Issues*, Martin J. Wainwright
- *High-Dimensional Statistics with a View Toward Applications in Biology*, Peter Bühlmann, Markus Kalisch, Lukas Meier
- *Next-Generation Statistical Genetics: Modeling, Penalization, and Optimization in High-Dimensional Data*, Kenneth Lange, Jeanette C. Papp, Janet S. Sinsheimer, Eric M. Sobel
- *Breaking Bad: Two Decades of Life-Course Data Analysis in Criminology, Developmental Psychology, and Beyond*, Elena A. Erosheva, Ross L. Matsueda, Donatello Telesca
- *Event History Analysis*, Niels Keiding
- *Statistical Evaluation of Forensic DNA Profile Evidence*, Christopher D. Steele, David J. Balding
- *Using League Table Rankings in Public Policy Formation: Statistical Issues*, Harvey Goldstein
- *Statistical Ecology*, Ruth King
- *Estimating the Number of Species in Microbial Diversity Studies*, John Bunge, Amy Willis, Fiona Walsh
- *Dynamic Treatment Regimes*, Bibhas Chakraborty, Susan A. Murphy
- *Statistics and Related Topics in Single-Molecule Biophysics*, Hong Qian, S.C. Kou
- *Statistics and Quantitative Risk Management for Banking and Insurance*, Paul Embrechts, Marius Hofert

Access this and all other Annual Reviews journals via your institution at www.annualreviews.org.

ANNUAL REVIEWS | Connect With Our Experts

Tel: 800.523.8635 (US/CAN) | Tel: 650.493.4400 | Fax: 650.424.0910 | Email: service@annualreviews.org

